

We are IntechOpen, the world's leading publisher of Open Access books Built by scientists, for scientists

6,900

Open access books available

186,000

International authors and editors

200M

Downloads

Our authors are among the

154

Countries delivered to

TOP 1%

most cited scientists

12.2%

Contributors from top 500 universities



WEB OF SCIENCE™

Selection of our books indexed in the Book Citation Index
in Web of Science™ Core Collection (BKCI)

Interested in publishing with us?
Contact book.department@intechopen.com

Numbers displayed above are based on latest data collected.
For more information visit www.intechopen.com



Functional MRI of Awake Behaving Macaques Using Standard Equipment

Reza Farivar and Wim Vanduffel

Additional information is available at the end of the chapter

<http://dx.doi.org/10.5772/31413>

1. Introduction

Functional magnetic resonance imaging (fMRI) is perhaps the most important development in the measurement of human brain function in recent neuroscience history. The technique allows for noninvasive whole-volume measurements of brain function in humans and repeatable non-invasive measurement of activity over the whole brain, providing a correlate of neural activity without use of tracers or electrodes. Well-developed commercial MRI systems with built-in support for functional imaging are widely available, as are a plethora of tools, both free and commercial, for the analysis of human functional brain images. The combination of non-invasiveness and the broad availability of equipment and tools to perform fMRI have made this technique popular and broadly adopted.

While human fMRI can go a long way to answering fundamental questions about organization of function in the brain, much of the information we obtain from fMRI is correlative—for example, while activity in an area may correlate with a task, it is impossible to assume that the activity *causes* the observed behaviour. In order to draw causal links between brain function and behavioural performance, it is necessary to directly alter the brain either prior to or during fMRI. While some coarse techniques exist to manipulate human brain function, such as transcranial magnetic stimulation, non-invasive methods comparable to localized chemical deactivations (Liu, Yttri et al. 2010) and local electrical microstimulation (Tolias, Sultan et al. 2005; Ekstrom, Roelfsema et al. 2008; Moeller, Freiwald et al. 2008; Ekstrom, Roelfsema et al. 2009) in the monkey do not exist for human imaging, and direct microstimulation or temporary deactivation by cortical infusion in a normal human subject is ethically unthinkable.

Studying brain function in humans alone is also limiting in that very little is known about the structure of the human brain—at least when compared to what we know about the macaque brain, for example. Axonal tracing requires local injection of a tracer molecule followed by

death and histological analysis, all of which is ethically infeasible in humans. In monkeys, this data has provided for a rich map of connectivity that can not only aid us in interpreting single-cell and fMRI results, but also formalize relationships between brain regions that can then be tested directly with temporary deactivation. For example, recently Schmid, Mrowka et al. (2010) used fMRI in awake-behaving macaques to demonstrate the neural basis for blind-sight—the residual visual capacity following loss of primary visual cortex (see (Leopold 2012 for a review). The anatomical basis for blind-sight has long been hypothesized to be the branching connections of the lateral geniculate nucleus of the thalamus (LGN) to other visual areas—in other words, while the V1 input to the cortical visual hierarchy is lost following ablation of V1, other visual areas receive indirect input via the thalamus. This hypothesis had not been directly tested, until Schmid et al. (2010)—that study was made possible by the fact that the projections of the LGN to the cortex are well known in the monkey.

Functional MRI in awake-behaving macaques thus affords us the possibility of studying primate brain function in a well-defined model (i.e., well-defined structure and connectivity) and to perturb the cortex using causal manipulations such as temporary deactivation, electrical microstimulation, or optogenetic manipulation (Boyden, Zhang et al. 2005; Gerits, Farivar et al. 2012). However, a number of challenges must be overcome to carry out a successful awake-behaving macaque fMRI study. Some aspects are general to animal neurophysiology studies—need for restraint, training, behavioural monitoring, etc.—while other aspects are unique to performing studies in the MRI scanner. These include the need to refrain from use of metallic material near the head, even if non-magnetic due to potential eddy current artifacts (Bernstein, King, et al. 2004), as well as issues pertaining to radio frequency (RF) noise, animal movement during scanning, motivation to perform specific behavioral tasks, environmental constraints for these tasks, etc. In this chapter, we begin with a comparison of human and monkey fMRI to highlight some of the differences and continue to discuss some of our solutions to the challenges of functional MRI with awake-behaving macaques. We close by discussing some unique possibilities afforded by fMRI in awake-behaving macaques.

1.1. Primate imaging and human comparison

A typical fMRI session with a human subject may follow this pattern: the participant is debriefed on both the experiment and aspects of the MR imaging, particularly noise issues and the importance of remaining still in the scanner. The participant's questions are answered and the experimenter, with the help of another individual typically, sets up the subject in a commercially available, clinical-grade head coil, places cushions around the subject's head and sometimes restrains the subject further by using a bite bar. The subject's behaviour may be monitored during the scanning as the subject tries to cooperate with the instructions given, and after each run, the experimenter talks with the subject to make sure all is well. During the scan, the subject does his utmost not to move and to pay attention to the task or stimuli, as requested by the experimenter.

A typical scan with an awake monkey may go a little differently: the experimenter restrains the monkey from his cage—good pole and collar training can go a long way to reduce this first step in a long line of frustrating steps. The animal is placed in an MR-compatible chair, and

his head is subsequently restrained using an implanted headpost that is then attached to the chair. Custom-made RF coils are then placed around the animal's head and tested on a vector network analyzer to ensure adequate performance. The animal is water restricted to increase its motivation to participate, but the level of motivation will vary depending on various factors, such as time of day being scanned, frequency of being scanned, amount of prior training in a simulator box, etc. During the scan, the animal receives juice reward for performing the required task, whether central fixation or more complicated tasks requiring response by way of eye movements or hand manipulations. While a well-trained monkey will perform this task well above 90% of the time, the animal will make many fast movements during a given scan. During some runs, for unclear reasons, the animal may choose not to behave according to training, and often after a short break, good behaviour returns to standard.

In short, a great deal changes between scanning humans and monkeys, and they begin with the fact that one has a cooperative human subject, and an innately uncooperative monkey who may do what you ask (most of the time) in return for juice. The monkey makes many more movements during a scan despite the fact that his head is rigidly fixed to the chair, and this has a strong negative influence on image and data quality, regardless of whether he performs his trained task.

1.2. Issues of particular relevance to imaging awake non-human primates

In this section, we will briefly discuss some of the demands of functional imaging in awake animals, and then discuss some of our solutions in meeting those demands.

First, we need a stable preparation. By stability we mean two different things—that the animal moves as little as possible, and that its performance during a scan is consistent. The movement of the animal requires means of head restraint that balance animal comfort with robust restraint against movements. Importantly, the means of head restraint must be fully MRcompatible, precluding use of metals anywhere near the brain. The head restraint method depends on a stable platform, typically the primate chair, which also needs to be non-magnetic and mechanically stable. The aspect of stability pertaining to the performance of the animal requires extensive training outside of the magnet which can last months to a year, depending on the specifics of the task, with conditions as comparable to the MRI conditions as possible— i.e. with simulated MRI noise at the same level as that of the MRI, same distance to screen, etc. The training regimen should also aim to create a stable pattern of performance for a reasonable amount of time (typically 2-6 hours). In other words, the animal should be occupied with a specific task throughout an entire scan, otherwise in absence of a task at hand, it may resort to fast movements which are detrimental to the quality of the images.

Second, we need high performance receive coils to pick up the small signal changes acquired during functional imaging scans. The coil design and layout are limited by the first requirement outlined above, namely that the coils must work around the head restraint employed. Importantly, given the drop in the signal-to-noise ratio (SNR) as a function of the distance between the coil and the subject (Mispelter, Lupu et al. 2006) the coils must be placed as close to the animal's head (brain) as possible. There is the added challenge of the monkey's jaw muscles that add considerable distance between the coils placed at the sides and the brain.

Third, we need to image at high spatial and temporal resolutions. Both require fast imaging methods which can be realized with high-speed and high-powered gradient systems and parallel imaging using phased array receive RF coils (Roemer, Edelstein et al. 1990; Kimmlingen, Eberlein et al. 2004). While standard gradients (i.e., $G \approx 45\text{mT/m}$ and $SR \approx 200\text{mT/m/s}$) on most 3-Tesla scanners can be sufficient to image volumes as small as $1.5 \times 1.5 \times 1.5\text{mm}$, faster ($>400\text{mT/m/s}$) and stronger ($>70\text{mT/m}$) gradients allow us to encode voxels as small as $0.5 \times 0.5 \times 0.5\text{mm}$ (Janssens, Keil et al. 2012; Kimmlingen, Eberlein et al. 2004). Multi-channel Phased array RF coils allow us to speed up the acquisition of a single image even further by acquiring multiple image fragments simultaneously (Roemer, Edelstein et al. 1990; Kimmlingen, Eberlein et al. 2004). These increases in speed and performance are important both to minimize image acquisition artifacts and to mitigate the effects of subject movement.

Finally, given that functionally-relevant signal fluctuations are a small ($<5\%$) of the overall signal and their fidelity may be further compromised by the increase in spatial and temporal resolution, we will need to find ways to enhance the strength of our functional signals. While some of this may be achieved through specific experimental designs, MR contrast agents—specifically MION (mono-iron oxide nanoparticles; Mandeville, Marota et al. 1998; Vanduffel, Fize et al. 2001, Leitte et al 2002)—can boost the functional signal drastically, by 3-4 fold at 3-Tesla.

1.3. Access to specialized equipment

A major appeal of our approach is that it does not require large-scale specialized equipment, such as a dedicated animal MRI. Our techniques can be easily incorporated in any standard clinical scanner, preferably 3-Tesla system with multiple receive channels. While dedicated animal-only MRI systems certainly have their own merit, the cost of such systems, above the costs of clinical-grade scanners that are available at many research facilities, prohibits their purchase by all but the wealthiest institutions.

2. Our approach

Below we outline the basic setup used for primate imaging in our group. We begin with a discussion of animal restraint because other aspects of the setup are restricted by this component.

2.1. Animal restraint

A now-common method of head restraint for neurophysiology studies involves attaching a metal post directly to the skull with titanium screws which tend to fuse to bone tissue (Betelak, Margiotti et al. 2001; Adams, Economides et al. 2007). Metallic objects close to the head would preclude any attempt to image the brain due to strong susceptibility artifacts (Matsuura, Inoue et al. 2005), and thus this method has been modified to make it appropriate for use in the MRI environment (Logothetis, Guggenberger et al. 1999; Vanduffel, Fize et al. 2001). In place of titanium screws, especially made ceramic screws (zirconia) are used that result in very little

noticeable susceptibility artifacts (Logothetis, Guggenberger et al. 1999; Scherberger, Fineman et al. 2003). The screws form a contact with the skull and the headpost is not directly held in place with these screws but instead it is embedded in acrylic that also embeds the ceramic screws. We have found that when used as a base material around the screws, a highly pure poly(methyl methacrylate) formulation (C & B METABOND) can result in a much more rigid and stable headpost preparation. In this way, a rigid connection is established between the headpost and skull (Betelak, Margiotti et al. 2001).

The head is then held in place using the headpost which is attached to the chair. The chair and the headpost holder are all made of non-metallic material, usually acrylic sheets and ultem components where rigidity and high tolerance against cracking is necessary—acrylic, while very rigid, cracks under force. Ultem components retain rigidity while being more resistant to cracking and breaking under pressure. It is important to note that several alternative methods of invasive head restraint have been proposed and used (e.g. Pigarev, Nothdurft et al. 1997; Keliris, Shmuel et al. 2007).

The design of the chair must take into account the placement of the RF coils, eye illumination, juice reward, as well as any other experimental attachments necessary. These items must be rigidly attached such that they interact very little with one another and are not disturbed by animal movements. As we will discuss further below, the rigidity of the RF coils is key to stable measurements, and the chair design must take this into consideration (AppliedPrototype 2011).

In our experience, an approach that balances animal comfort with strong restraint is key. Many researchers may find that too much restraint, such as additional restraint on limbs, may make the animal uncomfortable and result in reduced cooperation and thus performance. A welcomed contribution to this area is the development of non-invasive head-restraint methods, such as that recently developed by Srihasam and colleagues (Srihasam, Sullivan et al. 2010). This method does not require implanting of headposts while promising an adequate restraint on the head for animals without additional head apparatuses, such as recording wells.

2.2. Coil designs

Magnetic resonance signals are weak—the ratio of nuclei in the low energy state to high energy state, which is directly proportional to the strength of the measured resonance signal, is on the order of 0.0031% even at very high field strengths (e.g., 9.4T; De Graaf 2007, p. 7). This means that accurate and robust measurement of resonance signals requires sensitive RF coils. Coil sensitivity is affected by a number of factors, such as choice of conductor, size of the coil, and most importantly, distance of the coil to the brain. With reduced coil size (i.e., ~4cm diameter instead of >10cm diameter for human head coils) and close proximity to the brain (a tight-fitting coil rather than a one-size-fits-all helmet as used for humans), one can optimize coil sensitivity, but this comes at the cost of reduced field of view (FOV; e.g., Logothetis, Merkle et al. 2002). This reduced FOV is compensated by using an array of coils such that each coil becomes sensitive to one part of the brain, and the combination of all the coils together image the entire brain (Roemer, Edelstein et al. 1990). An added benefit of so-called multi-channel phased arrays is that image acquisition time can also be accelerated by a method analogous to

image-tiling (Pruessmann, Weiger et al. 1999; Sodickson, Griswold et al. 1999). While this does reduce the image SNR by up to 33% (Dietrich, Raya et al. 2007), it benefits us by allowing for faster imaging which (a) reduces image deformations, (b) allows us greater temporal resolution, and (c) grants us a greater degrees of freedom in our statistical analysis. In short, with parallel imaging we can make more measurements in less time with a small sacrifice in image SNR (de Zwart, van Gelderen et al. 2006).

We now almost exclusively use phased-array coils in our studies because of the advantages listed above. Phase-array coils for human applications typically make use of a helmet design for a complete sampling of the head (e.g., Wiggins, Triantafyllou et al. 2006), but in our experience helmet designs for monkeys pose difficulties due to obstruction by the headpost. In place of a helmet, a two-paddle design has many advantages, such as being easy to place over the head of many different monkeys and allowing them to be placed tightly around the head, thus maximizing the sensitivity of the coils. We now routinely use both 4-channel (two paddles with two channels each; e.g. Khachaturian 2010) and 8-channel coils (two paddles with 4 channels each), with the latter allowing for up to 3-fold acceleration as well. The receive channels are paired with a local transmit coil placed just above the head.

Because fMRI measurements can be heavily affected by temporal noise in addition to image SNR, it is imperative that the RF coils are rigidly placed so as to minimize movement or vibration (Roemer, Edelstein et al. 1990; Mispelter, Lupu et al. 2006). This applies to both the transmit coils and the receive channels. Vibration of the transmit coil can produce variations in the transmit field, adding temporal noise to our measurements (Mispelter, Lupu et al. 2006). Vibrations of the receive channels also adds temporal noise because movement of the receive coils away from the brain has the effect of changing the intensity of the signal detected by the coil, thus bringing about large changes in image intensity (Mispelter, Lupu et al. 2006). The receive channels are designed for use at a specific distance to the brain (Mispelter, Lupu et al. 2006), and changes in this distance will negatively affect the sensitivity of the coil which will result in both a decrease in signal and an increase in noise.

2.3. Sequence setup

The ideal functional imaging sequence would grant us high resolution, geometrically veridical images with high SNR at very short intervals. There is unfortunately a delicate balancing act as parameters that increase our resolution also decrease our SNR and prolong our imaging time while decreasing image veridicality. It is impossible to prescribe imaging parameters as this will vary depending on the setup at hand, the types of coils used (single loop or phased arrays), the performance of the gradients, the desired resolution, and finally, the type of signal measured. Discussion of these parameters is beyond the scope of this chapter, but a few general guidelines are helpful in animal imaging.

Given the size of the monkey brain as compared to the human brain (80 compared to 1250cm³; Gonen, Liu et al. 2008), voxel sizes used in humans (typically 2-3mm isotropic) would tend to be far too large for use in primate imaging as they would obstruct many small details of importance in the functional maps. While one may strive towards voxel sizes of 1mm or less, slightly above that is acceptable for imaging macaque brains. The size of the voxel is

dictated by the size of the imaging matrix, which in turn dictates how many voxels are to be measured in a given slice. Naturally, the larger the matrix size, the longer it will take to complete an image. The time to acquire one 2-D image depends on a number of factors, including matrix size, echo time, bandwidth, partial Fourier encoding, parallel imaging, amongst others (Bernstein, King et al. 2004). Thus it is not feasible to provide a formula to calculate acquisition time of one slice as it depends on a number of factors, many of which are also dependent on available hardware specifications. In general, however, increasing the matrix size increases echo time (TE) and the slice acquisition time—the increasing TE causes increased image blurring and image deformation and increasing slice acquisition time decreases temporal resolution (Bernstein, King et al. 2004). While for BOLD imaging at 3T the optimal TE is around 30 msec (Fera, Yongbi et al. 2004), with MION contrast agents, one can decrease the TE to below 20 msec (Leite, Tsao et al. 2002; Leite and Mandeville 2006), allowing for faster slice acquisition, which decreases image deformations and permits higher temporal resolutions.

Because even a well-restrained animal will move during acquisitions, the effect of movements on image acquisition must be carefully considered (Goense, Whittingstall et al. 2010). For example, as is typical of many fMRI studies, we routinely use interleaved acquisition whereby odd slices are acquired first prior to even slices. However, if an animal moves during single frame, then the odd and even slices are misaligned and standard 3d registration methods will be unable to correct for this. Worse, the misalignment can then propagate through the time series if slice-time correction is performed on the dataset (Sladky, Friston et al. 2011). Fortunately, a simple solution to this problem is to image in plane of head motion. For example, head restrained animals generally make very few lateral movements or rotations, but can use their bodies to push and pull their heads—thus the plane of motion is mainly sagittal. If one were to acquire horizontal or coronal slices, then such motion would pass through multiple slices and it would be impossible to visualize the motion and correct for them, since each slice is also acquired at a different time point. However, by acquiring sagittal slices, one can take optimal images of the movements and correct for them by applying 2-D slice-by-slice registration such as that offered by 2dImgReg of the AFNI toolset (Cox 1996). This correction can be done prior to slice-time correction so as to minimize the effects of head shifts in the sagittal plane on the rest of the dataset.

3. Preprocessing steps

A typical preprocessing stream for human functional data involves slice-time correction, 3D motion correction, and 3 Gaussian smoothing of the data prior to statistical analysis (Ashby 2011; Strother 2006). While the same steps may be used for processing of primate data, a few optimizations can be made.

As described above, by taking sagittal slices one can image the movements of the monkey head more adequately and correct for the 2-D movement using freely available tools from the AFNI toolkit (namely 2dImgReg). This software tool allows the specification of one image to serve

as the “base” image—an image where no motion was present between the two interleaved passes. Individual slices from the series are then registered to their target slice in this base image using only 2-D image registration. The result generates x,y and pitch rotation for each slice. Slice-based correction can improve 3-D registration because the latter cannot deal with situations where motion occurs during the acquisition of a volume and this can introduce errors in the 3-D correction (Kim, Boes et al. 1999). Thus while we have only begun to use 2-D in-plane realignment to correct for rapid head motion of the monkey, its utility has been previously demonstrated in human fMRI (Kim, Boes et al. 1999), although it is not widely used in that field.

Because it is customary to include motion-realignment parameters in the general linear model as nuisance variables, the output of 2-D in-plane registration per slice poses a problem because we typically have 50+ slices, and thus would have over a 150 parameters to include in our model. This impractical setup can be avoided by reducing the movement parameters using principal components analysis—since the motion in all the slices will likely be largely correlated, reducing them with principle components analysis will likely yield a good estimate of 2-D head motion that can then be used in the general linear model.

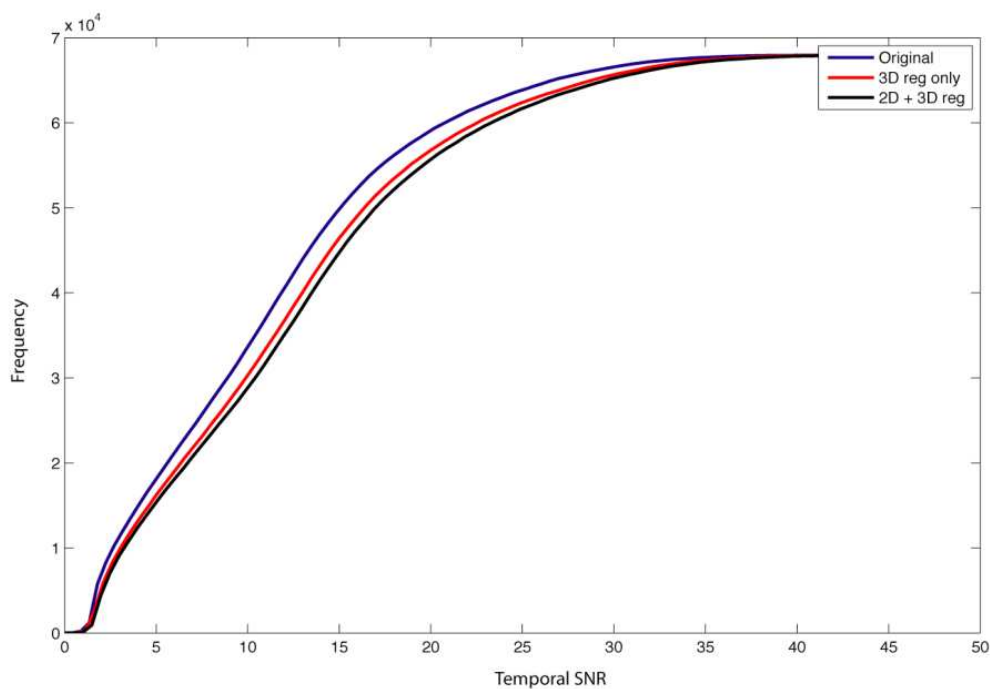


Figure 1. Cumulative histogram of voxel temporal SNR across different realignment strategies. The blue line depicts cumulative SNR without any motion correction. The red line depicts standard 3-D rigid motion correction, while the black line depicts the additional gain made by in-plane 2-D followed by 3-D rigid motion correction. 2-D in-plane registration can therefore improve temporal SNR, while the largest gain is made by 3-D rigid registration.

We can describe the potential sensitivity gain of such preprocessing steps by estimating temporal SNR, defined as time-course mean divided by time-course standard deviation

(Constantinides, Atalar et al. 1997). The cumulative histogram below (Figure 1) describes such a gain when using 2-D image realignment with sagittal slices followed by 3-D realignment, as opposed to the classic 3-D realignment typically performed. Over the entire volume of the brain (a crude measure), there is a gain of approximately 9% in temporal SNR by performing 3-D realignment, but this increases to an approximately 14% gain when it follows 2-D registration. Thus 2-D in-plane registration of sagittal slices followed by 3-D registration is a more appropriate strategy for image registration than classic 3-D realignment for motion correction.

Slice-time correction follows this 2-D motion correction because now the slices in the time series should be correctly aligned in space, permitting a meaningful correction to be performed in time. It is common to use sinc interpolation to correct for slice-time differences, but this method can propagate errors such as sudden changes in voxel values through the entire time series. It is thus advisable to use slower, more robust interpolators, such as Fourier or spline interpolators. Again, the AFNI tools offer a range of interpolators that can be used in place of sinc, as realized by the 3dTshift tool.

Three-dimensional movements, including lateral movements (if any) can then be corrected using any of a number of motion-correction tools—almost every package incorporates a motion correction algorithm, while a recent comparison (Oakes, Johnstone et al. 2005) suggests that those used by two of the more popular packages, namely SPM and AFNI, are quite comparable in performance, while the latter is substantially faster. Indeed, the AFNI tool 3dvolreg substantially outperforms SPM in 3-D motion realignment in speed and yields comparable results while not requiring the Matlab software package.

4. Functional-anatomical registration: Image deformation correction

Echo planar imaging (EPI), the method of choice for functional imaging, is prone to image deformations that can make the registration of the images to anatomical targets challenging (Farzaneh, Riederer et al. 1990; Andersson, Hutton et al. 2001). This is an issue that affects all EPI methods and animal imaging is no different. A number of solutions exist that either minimize deformations by acquiring segments of images more rapidly, or correct those deformations using informed or uninformed methods (i.e., using additional information about the imaging conditions obtained during the acquisition, or not).

First, a common method used to reduce deformation is to segment a single image into two or more pieces, and acquire each piece separately (Butts, Riederer et al. 1994). This method of segmented EPI is implemented prior to image reconstruction and involves acquiring interleaved lines of k -space in separate passes. The effect is that in each pass, very little time is spent acquiring the given lines, thus deformations are minimized. By acquiring multiple separate segments, the entire image is constructed out of minimally deformed acquisitions and the resulting image has high anatomical veridicality (Logothetis, Merkle et al. 2002; Goense, Whittingstall et al. 2010). The method, however, prolongs overall acquisition time substantially and is strongly vulnerable to even slight movements that would set the k -space lines out of alignment—thus it is very challenging to perform this with awake behaving animals. Using a

more conventional single-shot method, one could also acquire an entire image with a smaller matrix—thus a lower resolution—which would reduce deformations but the decreased resolution has many other disadvantages including reduced anatomical veridicality (Bernstein, King et al. 2004).

Because of the challenges of effectively reducing deformations at the acquisition side, a number of efforts have been made to correct for deformations after acquisition. Here, two categories of approaches can be considered—the informed and uninformed methods. An informed method makes use of independent additional information about the deformations, such as a field map (Jezzard and Balaban 1995; Andersson, Hutton et al. 2001) to correct for them. The main idea behind the field map method is to acquire another un-deformed image at the same resolution and position as the deformation-afflicted images, and then calculate the degree of deformation between the ideal and acquired images. This deformation field map can then be used to correct deformations in all the functional images. The field-map method has proven generally satisfactory in human imaging, but for animal imaging it poses a serious challenge because of the difficulty of making a stable field-map in an awake animal (see Jezzard 2012 for a review).

An interesting new development involves estimating deformations by measuring them in opposite directions (Holland, Kuperman et al. 2010). In echo-planar imaging, deformations are mostly in the phase-encoding direction (Jezzard and Balaban 1995). The method of Holland et al. (2010) involves acquiring two images in opposite phase-encoding directions. This means that each image will have deformation in the direction opposite to the other image (compression in one image will correspond to expansion in the other image). The balance between these two images would then be the un-deformed image, and the deformation map estimated from these two images can then be applied to the entire dataset. Furthermore, entire datasets or sessions can also be acquired in opposite phase-encoded directions to minimize imaging bias and combined so as to maximize overall image SNR— by combining minimally deformed voxels from forward and reverse phase-encoding directions.

4.1. 3-D Diffeomorphic demons correction

Image deformations can also be corrected by using the information available in the image itself in absence of secondary sources. In general, linear registration methods, such as affine registration methods that allow for translation, rotation, scale and shear, do not adequately correct for image deformations and one needs to make use of non-linear registration methods to achieve a good match between an EPI stack and an anatomical image. There are many non-linear methods that can be used to improve registration (for a review, see Zitova and Flusser 2003), but a danger of over-fitting is always present, as is the danger of creating new features—for example, if a gyrus in the functional image happens to fall closer to a sulcus after affine registration, some non-linear registration methods may force a dent in the gyrus to match the target image. We have found that non-linear registration using diffeomorphic demons (Vercauteren, Pennec et al. 2009) produces satisfactory and efficient results. The original demons algorithm (Thirion 1998) treats the registration problem as one of heat diffusion (an analogy to Maxwell's demons). In this formulation, the boundaries of the target image are

considered permeable membranes that allow for the diffusion of the source (moving) image through the permeable interfaces by effectors (agents) in the membrane or image contour. The source (moving) image is warped on a deformable grid, which maintains spatial relations between image elements. When combined with diffeomorphism (Chef d'Hotel, Hermosillo et al. 2002; Vercauteren, Pennec et al. 2009), which treats two images as manifolds with a differentiable one-to-one displacement field between them, the diffeomorphic demons algorithm (Vercauteren, Pennec et al. 2009) provides for an efficient non-linear multimodal (i.e., EPI to T1-weighted) registration method. This registration method ensures that the spatial order of voxels is maintained during registration, so as to prevent excessive compression or expansion of features in the image. Figure 2 demonstrates the advantage of 3-D diffeomorphic registration of an EPI volume to an anatomical target, as opposed to a 12-parameter affine registration.

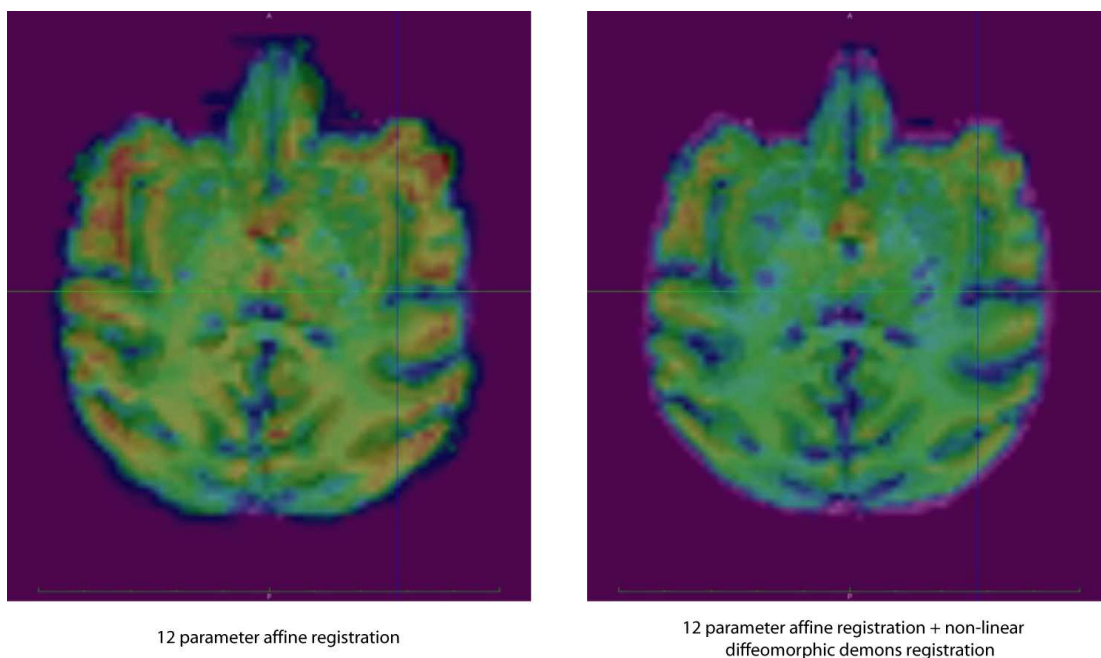


Figure 2. Comparison of 12-parameter affine registration (translation (x,y,z), rotation (pitch, roll, yaw), scale (ax,ay,az) and shear across x,y & z) with or without non-linear diffeomorphic registration for an EPI acquired with left-right phase encoding. The areas in red are regions that are poorly registered.

While EPI images in general have a very different contrast compared to MPRAGE anatomical images, images acquired with MION are even more different. This mismatch of the intensity distributions in the image can negatively affect the image registration. Hence it is useful to either use a mutual-information minimization strategy that avoids intensitybased matching, or modify the contrast profile of the T1-weighted anatomical such that it has a contrast comparable to the MION EPI images. In other words, we substitute a different image intensity look-up table such that the T1-weighted image looks more similar to a MION EPI image. The contrast profile or look-up table of an image may be modified through any of a number of image processing tools, including the Image Processing toolbox in Matlab or with the freely available Slicer package and its Histogram Matching module.

5. Statistical analysis

For the most part, statistical analysis of macaque functional images follows the same methods as those used in human imaging (Friston, Holmes et al. 1995). Specifically, the general linear model is used to make estimates of differential brain activity by convolving a known impulse response function, in our case the MION response function (Leite, Tsao et al. 2002; Leite and Mandeville 2006), with the onset of the stimulation events and adjusted for the duration of those events. The model response profile for all conditions are then fitted to the high-pass filtered data and the beta values estimated for two conditions are compared and tested for statistical significance with various corrections in place to reduce the possibility of Type I errors, such as Bonferroni correction, Gaussian Random Field (Worsley and Friston 1995), or false discovery rate (Benjamini and Hochberg 1995). However, a few additional steps can go a long way to decrease Type II errors and increase our statistical power, and these are discussed below.

5.1. Artifact rejection

The most overlooked but important aspect of functional image analysis is to simply look at the raw data and verify data quality. This may come as a daunting task, given the seemingly large amount of data. Yet a number of popular packages offer very simple methods of quickly assessing data quality with visual inspect and/or by quantitative methods. For example, the volume viewer in the FSL package (`fslview`) allows one to quickly load and animate through an entire functional volume time series while checking through in multiple orthogonal views for artefacts. The AFNI viewer allows one to rapidly click through voxels to visually check for unexpected signal changes. It is almost a fact that image fluctuations will occur when working with an awake and behaving animal, but the severity of the changes can be quickly assessed with these tools. Indeed, it is of great value to familiarize oneself with these tools to also evaluate the efficacy of the entire preprocessing stream.

A number of formal methods can be used to select and remove outliers from the dataset on the basis of additional data, such as behaviour of the animal, or based on movement estimates obtained from motion-correction tools (Goense, Whittingstall et al. 2010). In general it is preferable to exclude “bad” volumes from the analysis rather than correct for them, because the degree and effectiveness of any correction is hard to evaluate and indeed, some “corrections” may actually add more noise to the data than they remove. At least both AFNI’s and SPM’s GLM analysis tools (the latter via the ART repair toolkit; Mazaika, Hoefft et al. 2009) allows for exclusion of outliers. The ART repair tool readily allows for exclusion (or de-weighting) of the outlier volumes from the GLM analysis, with outliers selected on the basis of movement parameters and average signal intensity. In contrast, AFNI’s GLM tool, `3dDeconvolve`, allows for exclusion of volumes on any basis, allowing the experimenter to select volumes based on external measurements such as animal behaviour as well as on image realignment parameters, etc.

5.2. Behavioural and motion regressors

The exclusion of outliers can have drastic effects on reducing the noise in a dataset. Another approach is to reduce non-white noise by providing estimates of noise sources and incorporating this in the GLM analysis as regressors of no interest (Friston, Williams et al. 1996; Lund, Madsen et al. 2006). It is common and quite effective to include movement estimates obtained during motion correction in the GLM model. Additional regressors can be included, such as behaviours of no interest (e.g. saccades made during a fixation task) or external estimates of motion or jaw movement. A challenge with including regressors of no interest is that one does not know a priori how the regressors correspond to changes in voxel intensity values. For example, head movements will likely affect voxel values, but whether the direction of change or its magnitude or even its pattern would correspond to the movement estimates is not clear. In general, inclusion of additional estimates of noise sources does reduce variability in a dataset and is therefore recommended.

An approach that we are currently investigating is the inclusion of variability estimates obtained from non-brain tissue. In this approach, a brain mask is inverted to only select nonbrain voxels. Using principle components analysis, we then estimate a limited number of components that explain the majority of non-brain time-course variance. Finally, we include these estimates as regressors of no interest in the GLM analysis. In effect, we treat non-brain tissue as samples of noise, and estimate the main sources of this noise by reducing the data with principle components analysis. We assume that there are fewer noise sources than nonbrain voxels, and that the various noise sources result in correlated extraneous signals across multiple voxels. Based on these assumptions, we can then seek to estimate the noise sources by estimating principle components of the time-course of non-brain voxels, which will highlight noise components that may be distributed across a number of voxels. Noise signals may arise from eye, head, or jaw movement, or instabilities in the RF coil. The figure below (Figure 3) describes the amount of variance explained in the brain by non-brain components. Note that the components well capture the large fluctuations in the jaw muscles and the eyes, but also capture a significant amount of variability in the brain. This method is still under investigation, but it seems a quite promising method to reduce variability in time course data.

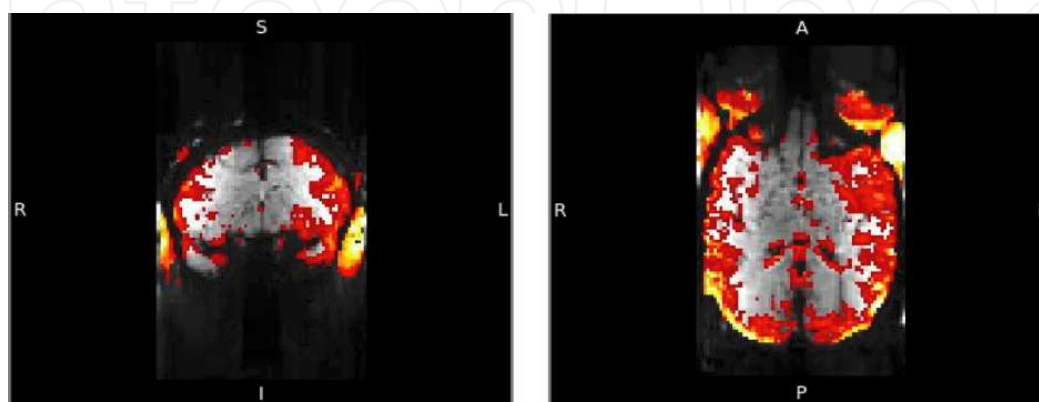


Figure 3. Variance explained by 20 non-brain principle components (corrected FWE < 0.05)

5.3. Experimental design strategies to minimize movement of an uncooperative animal subject

A major challenge of working with animals is that one has to motivate them to perform the task at hand. Typically this is done by restricting their fluid intake so that they are motivated to work for a liquid reward during the scans. However, even then it can be difficult or impossible to completely ensure the animal complies with the experimenter's wishes. The optimal solution involves motivating the animal so that it works for fluids, habituating it to the scanner environment by training it frequently in a simulated scanner environment, and minimizing the effect that its movements can have on the experiment itself. We routinely habituate our animals for months before the actual scans, and even then they are habituated in the scanner for a number of scans before their performance compares to that obtained outside of the scanner. The animal restraint, as discussed above, must be balanced against animal comfort given that the animal may be restrained for several hours at a time.

6. Combining methods with fMRI

While functional imaging in macaques bridges a crucial gap in comparing the function of human and non-human primate brains (Vanduffel, Fize et al. 2002; Orban, Fize et al. 2003; Orban, Claeys et al. 2005; Nelissen, Vanduffel et al. 2006; Kolster, Mandeville et al. 2009), a major advantage of working with an animal model is the ability to directly manipulate the brain to assess the causal interactions of brain networks. Our lab and others have now successfully implemented electrical microstimulation of the brain simultaneous with functional imaging to assess the role of FEF microstimulation on the cortical response to simple and complex visual stimuli (Ekstrom, Roelfsema et al. 2008; Ekstrom, Roelfsema et al. 2009), stimulation of face-selective patches in the macaque cortex (Moeller, Freiwald et al. 2008) and role of microstimulation in the propagation of information in the cortex more generally (Tolias, Sultan et al. 2005; Logothetis, Augath et al. 2010). The information obtained by this combination could not have been garnered using other methods, such as single-unit recordings, as this would require simultaneously measuring over large swaths of cortex—a task that is virtually impossible.

Another important development is the temporary deactivation of a brain area to assess its role in a more complex network. The application of muscimol, a GABA agonist, to temporarily shut down an area is now common and many labs have successfully applied this to measure the effect of deactivation on behaviour and single-unit responses. Our lab has now extended this to use with fMRI to allow us to measure both the brain response and its correlated behavioural change (Gerits, Wardak et al. 2009).

In addition to temporary deactivation, a number of groups have successfully combined local cortical lesions with fMRI. Pinsk, Moore, et al. (2005) were first to demonstrate feasibility of performing fMRI in awake-behaving macaques with striate cortex lesions. Lesions to the striate cortex in humans lead to a phenomenon termed "blindsight" (see Leopold, 2012, for a

recent review). Blindsight patients are essentially unaware of visual stimulation, yet they are able to respond to such stimuli without conscious awareness. Pinsk, Moore et al. (2005) were first to demonstrate that following striate cortex lesions, the extrastriate visual cortex continues to be responsive to visual stimuli as measured by fMRI. This finding was later corroborated by Schmid, Panagiotaropoulos et al. (2009) who showed that V2 and V3 in awake-behaving macaques with focal striate lesions continue to be responsive to visual stimulation, albeit at 70% the pre-lesion rate, when measured with fMRI. They further demonstrated that retinotopy in V2 and V3 corresponding to the lesion in V1 did not change, suggesting that post-lesion activity in these areas was not driven by peri-lesion V1. This further highlighted the possibility that blindsight is mediated by sub-cortical inputs. Schmid et al (2010) provided the conclusive evidence that blindsight is mediated by sub-cortical inputs to extrastriate cortex—specifically the LGN. Using fMRI in awake-behaving macaques with striate lesions, they first corroborated earlier findings of Pinsk et al (2005) and Schmid et al. (2009) and demonstrated that extrastriate cortex remains active following striate cortex, but at a lower level. They then temporarily deactivated the LGN with a GABA agonist while measuring the responses of the visual cortex of the macaques using fMRI. They found that deactivation of the LGN in striate-lesioned macaques completely abolished the residual response of the extrastriate cortex to visual inputs as well as residual behavioural function. This was the first direct evidence that projections from LGN to extrastriate cortex allow for blindsight to occur, and demonstrates the power of combining fMRI with causal manipulations to answering fundamental questions in systems neuroscience.

An exciting new development by our group is the integration of optogenetic methods (Boyden, Zhang et al. 2005) with fMRI in awake-behaving macaques (Gerits, Farivar et al. 2012). We have demonstrated that optogenetic stimulation of the frontal eye fields results in activation in a number of cortically-connected nodes, and for the first time, that optogenetic stimulation in primates can affect behavioural performance—in our case, saccade latency in a visually-guided task (Gerits, Farivar et al. 2012). These results are important for the further development and refinement of optogenetic methods to select sub-population of neurons in the cortex and evaluate their contribution to global brain activity as well as behaviour.

While fMRI provides images of population neural activity based on indirect measures, it is possible to combine it with simultaneous electrophysiological recordings (Logothetis, Pauls et al. 2001; Logothetis, Kayser et al. 2007; Oeltermann, Augath et al. 2007). This combination helps overcome an important challenge in interpreting the fMRI response and provide a confirmation and an additional metric of the underlying neural processes. However, a more practical approach is to use fMRI to guide subsequent electrophysiology outside of the MRI (e.g. Tsao, Freiwald et al. 2006; Freiwald and Tsao 2010). Of course, this does not allow for direct links to be made between BOLD signal fluctuations and underlying spiking activity, but it does allow for more refined examination of a patch of tissue identified by fMRI using single-cell recordings.

7. Impact and future directions

Functional MRI is useful for measuring activity over the whole brain, for identifying regions of importance for subsequent analysis, for assessing brain-wide effects of lesions, deactivations, or selected stimulations. Performing fMRI in awake-behaving macaques is not trivial and requires reconsideration of a number of factors, including restraint, training, coil design, image acquisition, data pre-processing, and additional refinements of the statistical analysis steps. Implementation of the solutions described above contributes to the feasibility of performing fMRI in awake-behaving macaques, which opens the door to answering a large number of questions in systems neuroscience. The power of this utility is best realized when combined with temporary causal manipulations of cortical function, such as combining with electrical or optogenetic stimulation or with temporary and/or permanent deactivation, or in conjunction with single-cell recordings to understand in detail the contribution of single cell responses to behavioural outcomes.

Author details

Reza Farivar^{1,2} and Wim Vanduffel^{1,3}

1 Massachusetts General Hospital and Harvard Medical School, USA

2 McGill Vision Research Unit, McGill University, Canada

3 Katholieke Universiteit Leuven, Belgium

References

- [1] Adams, D. L., J. R. Economides, et al. (2007). "A biocompatible titanium headpost for stabilizing behaving monkeys." *J Neurophysiol* 98(2): 993-1001.
- [2] Andersson, J. L., C. Hutton, et al. (2001). "Modeling geometric deformations in EPI time series." *Neuroimage* 13(5): 903-919.
- [3] Applied Prototype. (2011). "Vanduffel/HMS fMRI chair." from <http://appliedprototype.com/AppliedPrototype/Vanduffel.html>.
- [4] Ashby, F. G. (2011). *Statistical analysis of fMRI data*. Cambridge, Mass., MIT Press.
- [5] Benjamini, Y. and Y. Hochberg (1995). "Controlling the false discovery rate: A practical and powerful approach to multiple testing." *Journal of the Royal Statistical Society, Series B (Methodological)* 57: 289-300.

- [6] Bernstein, M. A., K. F. King, et al. (2004). Handbook of MRI pulse sequences. Amsterdam ; Boston, Academic Press.
- [7] Betelak, K. F., E. A. Margiotti, et al. (2001). "The use of titanium implants and prosthodontics techniques in the preparation of non-human primates for long-term neuronal recording studies." *J Neurosci Methods* 112(1): 9-20.
- [8] Boyden, E. S., F. Zhang, et al. (2005). "Millisecond-timescale, genetically targeted optical control of neural activity." *Nat Neurosci* 8(9): 1263-1268.
- [9] Butts, K., S. J. Riederer, et al. (1994). "Interleaved echo planar imaging on a standard MRI system." *Magn Reson Med* 31(1): 67-72.
- [10] Chef d'Hotel, C., G. Hermosillo, et al. (2002). Flows of diffeomorphisms for multimodal image registration. *IEEE International Symposium on Biomedical Imaging*. Constantinides, C. D., E. Atalar, et al. (1997). "Signal-to-noise measurements in magnitude images from NMR phased arrays." *Magn Reson Med* 38(5): 852-857.
- [11] Cox, R. W. (1996). "AFNI: software for analysis and visualization of functional magnetic resonance neuroimages." *Comput Biomed Res* 29(3): 162-173.
- [12] De Graaf, R. A. (2007). *In vivo NMR spectroscopy : principles and techniques*. Chichester, West Sussex, England ; Hoboken, NJ, John Wiley & Sons.
- [13] de Zwart, J. A., P. van Gelderen, et al. (2006). "Accelerated parallel imaging for functional imaging of the human brain." *NMR Biomed* 19(3): 342-351.
- [14] Dietrich, O., J. G. Raya, et al. (2007). "Measurement of signal-to-noise ratios in MR images: influence of multichannel coils, parallel imaging, and reconstruction filters." *J Magn Reson Imaging* 26(2): 375-385.
- [15] Ekstrom, L. B., P. R. Roelfsema, et al. (2008). "Bottom-up dependent gating of frontal signals in early visual cortex." *Science* 321(5887): 414-417.
- [16] Ekstrom, L. B., P. R. Roelfsema, et al. (2009). "Modulation of the contrast response function by electrical microstimulation of the macaque frontal eye field." *J Neurosci* 29(34):10683-10694.
- [17] Farzaneh, F., S. J. Riederer, et al. (1990). "Analysis of T2 limitations and off-resonance effects on spatial resolution and artifacts in echo-planar imaging." *Magn Reson Med* 14(1): 123-139.
- [18] Fera, F., M. N. Yongbi, et al. (2004). "EPI-BOLD fMRI of human motor cortex at 1.5 T and 3.0 T: sensitivity dependence on echo time and acquisition bandwidth." *J Magn Reson Imaging* 19(1): 19-26.
- [19] Freiwald, W. A. and D. Y. Tsao (2010). "Functional compartmentalization and viewpoint generalization within the macaque face-processing system." *Science* 330(6005): 845-851.

- [20] Friston, K. J., A. P. Holmes, et al. (1995). "Statistical parametric maps in functional imaging: A general linear approach." *Human Brain Mapping* 2(4): 189-210.
- [21] Friston, K. J., S. Williams, et al. (1996). "Movement-related effects in fMRI time-series." *Magn Reson Med* 35(3): 346-355.
- [22] Gerits, A., C. Wardak, et al. (2009). Behavioral and brain-wide functional consequences of reversible LIP inactivation during visual search. Society for Neuroscience Annual Meeting, Chicago, IL, Online.
- [23] Gerits, A., R. Farivar, et al. (2012). "Optogenetically Induced Behavioral and Functional Network Changes in Primates." *Curr Biol*.
- [24] Goense, J. B., K. Whittingstall, et al. (2010). "Functional magnetic resonance imaging of awake behaving macaques." *Methods* 50(3): 178-188.
- [25] Gonen, O., S. Liu, et al. (2008). "Proton MR spectroscopic imaging of rhesus macaque brain in vivo at 7T." *Magn Reson Med* 59(4): 692-699.
- [26] Hackensack, NJ, Imperial College Press ; Distributed by World Scientific.
- [27] Holland, D., J. M. Kuperman, et al. (2010). "Efficient correction of inhomogeneous static magnetic field-induced distortion in Echo Planar Imaging." *Neuroimage* 50(1): 175-183.
- [28] Janssens, T., B. Keil, et al. (2012). "An implanted 8-channel array coil for high-resolution macaque MRI at 3T." *Neuroimage* 62(3): 1529-1536.
- [29] Jezzard, P. (2012). "Correction of geometric distortion in fMRI data." *Neuroimage* 62(2): 648-651.
- [30] Jezzard, P. and R. S. Balaban (1995). "Correction for geometric distortion in echo planar images from B0 field variations." *Magn Reson Med* 34(1): 65-73.
- [31] Keliris, G. A., A. Shmuel, et al. (2007). "Robust controlled functional MRI in alert monkeys at high magnetic field: effects of jaw and body movements." *Neuroimage* 36(3): 550-570.
- [32] Khachaturian, M. H. (2010). "A 4-channel 3 Tesla phased array receive coil for awake rhesus monkey fMRI and diffusion MRI experiments." *J Biomed Sci Eng* 3(11): 1085-1092.
- [33] Kim, B., J. L. Boes, et al. (1999). "Motion correction in fMRI via registration of individual slices into an anatomical volume." *Magn Reson Med* 41(5): 964-972.
- [34] Kimmlingen, R., E. Eberlein, et al. (2004). An easy to exchange high performance head gradient insert for a 3T whole body MRI system: First results. Proceedings of International Society for Magnetic Resonance Medicine. 11.
- [35] Kolster, H., J. B. Mandeville, et al. (2009). "Visual field map clusters in macaque extrastriate visual cortex." *J Neurosci* 29(21): 7031-7039.

- [36] Leite, F. P. and J. B. Mandeville (2006). "Characterization of event-related designs using BOLD and IRON fMRI." *Neuroimage* 29(3): 901-909.
- [37] Leite, F. P., D. Tsao, et al. (2002). "Repeated fMRI using iron oxide contrast agent in awake, behaving macaques at 3 Tesla." *Neuroimage* 16(2): 283-294.
- [38] Leopold, D. A. (2012). "Primary visual cortex: awareness and blindsight." *Annu Rev Neurosci* 35: 91-109.
- [39] Liu, Y., E. A. Yttri, et al. (2010). "Intention and attention: different functional roles for LIPd and LIPv." *Nat Neurosci* 13(4): 495-500.
- [40] Logothetis, N. K., C. Kayser, et al. (2007). "In vivo measurement of cortical impedance spectrum in monkeys: implications for signal propagation." *Neuron* 55(5): 809-823.
- [41] Logothetis, N. K., H. Guggenberger, et al. (1999). "Functional imaging of the monkey brain." *Nat Neurosci* 2(6): 555-562.
- [42] Logothetis, N. K., J. Pauls, et al. (2001). "Neurophysiological investigation of the basis of the fMRI signal." *Nature* 412(6843): 150-157.
- [43] Logothetis, N. K., M. Augath, et al. (2010). "The effects of electrical microstimulation on cortical signal propagation." *Nat Neurosci* 13(10): 1283-1291.
- [44] Logothetis, N., H. Merkle, et al. (2002). "Ultra high-resolution fMRI in monkeys with implanted RF coils." *Neuron* 35(2): 227-242.
- [45] Lund, T. E., K. H. Madsen, et al. (2006). "Non-white noise in fMRI: does modelling have an impact?" *Neuroimage* 29(1): 54-66.
- [46] Mandeville, J. B., J. J. Marota, et al. (1998). "Dynamic functional imaging of relative cerebral blood volume during rat forepaw stimulation." *Magn Reson Med* 39(4): 615-624.
- [47] Matsuura, H., T. Inoue, et al. (2005). "Quantitative analysis of magnetic resonance imaging susceptibility artifacts caused by neurosurgical biomaterials: comparison of 0.5, 1.5, and 3.0 Tesla magnetic fields." *Neurol Med Chir (Tokyo)* 45(8): 395-398; discussion 398-399.
- [48] Mazaika, P., F. Hoeft, et al. (2009). *Methods and Software for fMRI Analysis for Clinical Subjects*. Human Brain Mapping.
- [49] Mispelter, J., M. Lupu, et al. (2006). *NMR probeheads for biophysical and biomedical experiments : theoretical principles & practical guidelines*. London
- [50] Moeller, S., W. A. Freiwald, et al. (2008). "Patches with links: a unified system for processing faces in the macaque temporal lobe." *Science* 320(5881): 1355-1359.

- [51] Nelissen, K., W. Vanduffel, et al. (2006). "Charting the lower superior temporal region, a new motion-sensitive region in monkey superior temporal sulcus." *J Neurosci* 26(22): 5929-5947.
- [52] Oakes, T. R., T. Johnstone, et al. (2005). "Comparison of fMRI motion correction software tools." *Neuroimage* 28(3): 529-543.
- [53] Oeltermann, A., M. A. Augath, et al. (2007). "Simultaneous recording of neuronal signals and functional NMR imaging." *Magn Reson Imaging* 25(6): 760-774
- [54] Orban, G. A., D. Fize, et al. (2003). "Similarities and differences in motion processing between the human and macaque brain: evidence from fMRI." *Neuropsychologia* 41(13): 1757-1768.
- [55] Orban, G. A., K. Claeys, et al. (2005). "Mapping the parietal cortex of human and non-human primates." *Neuropsychologia*.
- [56] Pigarev, I. N., H. C. Nothdurft, et al. (1997). "A reversible system for chronic recordings in macaque monkeys." *J Neurosci Methods* 77(2): 157-162.
- [57] Pinsk, M. A., T. Moore, et al. (2005). "Methods for functional magnetic resonance imaging in normal and lesioned behaving monkeys." *J Neurosci Methods* 143(2): 179-195.
- [58] Pruessmann, K. P., M. Weiger, et al. (1999). "SENSE: sensitivity encoding for fast MRI." *Magn Reson Med* 42(5): 952-962.
- [59] Roemer, P. B., W. A. Edelstein, et al. (1990). "The NMR phased array." *Magn Reson Med* 16(2): 192-225.
- [60] Scherberger, H., I. Fineman, et al. (2003). "Magnetic resonance image-guided implantation of chronic recording electrodes in the macaque intraparietal sulcus." *J Neurosci Methods* 130(1): 1-8.
- [61] Schmid, M. C., S. W. Mrowka, et al. (2010). "Blindsight depends on the lateral geniculate nucleus." *Nature* 466(7304): 373-377.
- [62] Schmid, M. C., T. Panagiotaropoulos, et al. (2009). "Visually driven activation in macaque areas V2 and V3 without input from the primary visual cortex." *PLoS One* 4(5): e5527.
- [63] Sladky, R., K. J. Friston, et al. (2011). "Slice-timing effects and their correction in functional MRI." *Neuroimage*.
- [64] Sodickson, D. K., M. A. Griswold, et al. (1999). "Signal-to-noise ratio and signal-to-noise efficiency in SMASH imaging." *Magn Reson Med* 41(5): 1009-1022.
- [65] Srihasam, K., K. Sullivan, et al. (2010). "Noninvasive functional MRI in alert monkeys." *Neuroimage* 51(1): 267-273.

- [66] Strother, S. C. (2006). "Evaluating fMRI preprocessing pipelines." *IEEE Eng Med Biol Mag* 25(2): 27-41.
- [67] Thirion, J. P. (1998). "Image matching as a diffusion process: an analogy with Maxwell's demons." *Med Image Anal* 2(3): 243-260.
- [68] Tolias, A. S., F. Sultan, et al. (2005). "Mapping cortical activity elicited with electrical microstimulation using FMRI in the macaque." *Neuron* 48(6): 901-911.
- [69] Tsao, D. Y., W. A. Freiwald, et al. (2006). "A cortical region consisting entirely of face-selective cells." *Science* 311(5761): 670-674.
- [70] Vanduffel, W., D. Fize, et al. (2001). "Visual motion processing investigated using contrast agent-enhanced fMRI in awake behaving monkeys." *Neuron* 32(4): 565-577.
- [71] Vanduffel, W., D. Fize, et al. (2002). "Extracting 3D from motion: differences in human and monkey intraparietal cortex." *Science* 298(5592): 413-415.
- [72] Vercauteren, T., X. Pennec, et al. (2009). "Diffeomorphic demons: efficient non-parametric image registration." *Neuroimage* 45(1 Suppl): S61-72.
- [73] Wiggins, G. C., C. Triantafyllou, et al. (2006). "32-channel 3 Tesla receive-only phased-array head coil with soccer-ball element geometry." *Magn Reson Med* 56(1): 216-223.
- [74] Worsley, K. J. and K. J. Friston (1995). "Analysis of fMRI time-series revisited--again." *Neuroimage* 2(3): 173-181.
- [75] Zitova, B. and J. Flusser (2003). "Image registration methods: a survey." *Image and Vision Computing* 21(11): 977-1000.

